Sol-gel derived scheelite-type LiEuW$_2$O$_8$ red phosphor for white light emitting diodes

KYU-SEOG HWANG[a*], SEUNG-HWANGBO[b], JIN-TAE KIM[c]

[a]*Department of Biomedical Engineering, Nambu University, 864-1 Wolgye-dong, Gwangsan-gu, Gwangju 506-824, Korea*
[b]*Major in Photonic Engineering, Division of Electronic & Photonic Engineering, Honam University, 59-1 Seobong-dong, Gwangsan-gu, Gwangju 506-714, Korea*
[c]*Department of Photonic Engineering, College of Engineering, Chosun University, 375 Seosuk-dong, Dong-gu, Gwangju 501-759, Korea*

LiEuW$_2$O$_8$ phosphors with the optical function of color conversion from near-UV to red were prepared by sol-gel method using a lithium acetate dehydrate, europium(III) nitrate pentahydrate, and tungsten(VI) chloride as a starting materials. Viscous mixing sol was pyrolyzed at 200, 250 and 300°C for 120 min in air and then white powder precursor was finally annealed at 700°C for 240 min in Ar. Crystallinity, surface morphology, and photoluminescent properties are investigated by an X-ray diffraction analysis, field emission – scanning electron microscope and a fluorescent spectrophotometer. The characteristic emission of WO$_4^{-2}$ in LEW is quenched absolutely and only red-light emission of Eu^{3+} appears. Crystallinity, surface properties and red-emission by near-ultraviolet (395 nm) were improved by high-temperature pyrolysis.

1. Introduction

White LED can be obtained by combining a InGaN blue LED emitting at 465 nm with a broad-band yellow phosphor, e.g., Y$_3$Al$_5$O$_{12}$:Ce^{3+} (YAG:Ce) [1 - 3]. However, it has problems of low color stability with increasing applied current, low color rendering index, and low color reproducibility.

Recently, white LEDs fabricated by red/green/blue tricolor phosphors with near-ultraviolet (UV) Ga(In)N chips have been considered as the most efficient method because near-UV lights almost place little effect on the color quality. That is to say, they can reproduce full color that all color points fall inside the MacAdam oval. And they are also entitled to high output and stability [4, 5].

However, the efficiency of the commercially available red phosphors, Y$_2$O$_2$S:Eu^{3+} for blue and near-UV GaN based LED, is about eight times less than that of the blue and green phosphors, and this sulfide-based phosphor is chemically unstable. For achieving the three phosphors-converted white LED, it is imperative to develop new effective red phosphors suitable for near-UV LED chips. Therefore, lack of proper red phosphors becomes the bottleneck for the SSL (Solid state lighting) devices.

Recently, much attention has been paid to make superior red phosphor for white LED. Previously reported scheelite-type compound, LiEuW$_2$O$_8$ (LEW), can be written as ABM$_2$O$_8$ (A: monovalent metal, B: trivalent rare earth, M: Mo$_{6+}$ or W$_{6+}$), exhibits high red emission

efficiency under excitation of blue light [6]. LEW has attractive photoluminescent properties; i) the red emission due to 4f-4f transition of Eu^{3+} when excited by UV, blue or green light, ii) concentration quenching hardly occurs in scheelite-type LEW [7 - 9]. This weak concentration quenching property is known to be due to the W-O covalent bond [7 – 9].

Most of LEW was produced from metal oxides by conventional solid-state reaction at above 1000°C [10]. As far as we know, there is a little information on the successful sol-gel synthesis of LEW red phosphor.

In this work, we prepared LEW phosphors with the optical function of color conversion from near-UV to red by sol-gel method. Since, for the chemical-solution-based process such as sol-gel, the properties of final product were largely affected by the organics in precursor, it is very important to recognize the relation between the pyrolysis temperature and the properties of the annealed sample. Effect of organics in precursor on crystallographical, morphological and optical properties was investigated as a function of pre-firing temperature.

2. Experimental

For the synthesis of LEW, stoichiometric mixtures of lithium acetate dehydrate (C$_2$H$_3$LiO$_2$·2H$_2$O), europium(III) nitrate pentahydrate [Eu(NO$_3$)$_3$·5H$_2$O], and tungsten(VI) chloride (WCl$_8$) were dissolved with H$_2$O$_2$ and iso-

propanol, respectively. A weighed quantity of urea (NH$_2$CONH$_2$) was added to the solution at 100°C. The molar ratio of urea to the total concentration of metal ions was adjusted to 1.5. After mixing, homogeneous colorless solution was obtained. The solvent was slowly evaporated off from solution at 100°C and a colorless precursor with high viscosity was obtained. Subsequently the precursor prefired in a dry oven at 200, 250 and 300°C for 120 min in air to obtain white powder. Finally the dried powder was annealed in a tube furnace at 700°C for 240 min in Ar (heating rate: 3°C/min).

Thermogravimetric-differential thermal analysis (TG-DTA, DTG-60, Shimadzu, Japan) of the starting sol was performed using an α-alumina reference and a heating rate 3K/min. X-ray diffraction profiles were measured using an X-ray diffractometer (XRD, D-Max-1200, Rigaku, Japan), equipped with a CuKα radiation source and a graphite monochrometer. Particle size and shapes were observed by field emission – scanning electron microscope (FE-SEM, S-4700, Hitachi, Japan). The excitation and emission spectra were recorded on a fluorescent spectrophotometer (F4500, Hitachi, Japan).

3. Results and discussion

The TG-DTA curves of the starting sol were studied, as shown in Fig. 1, to understand its pyrolysis behavior and crystallization process. Fig. 1 shows that the weight loss of the starting sol occurs in the TG curve with the increase of temperature from room temperature to 300°C. The first weight loss occurred below 200°C in the TG curve, which was attributed to the removal of surface absorbed water. The second weight loss step occurred between 200 and 300°C, which was attributed to the burning of the organics. Thereafter, the weight remains constant, which indicates that the decomposition and combustion of all organics in the starting sol have been completed below 300°C. The exothermic peak in DTA curve at about 250°C is ascribed to combustion and the formation of the LEW nuclei. As seen in Fig. 1, the temperatures of 200°C and 250°C correspond to the initial and intermediate stage of the pyrolysis. The weight decrease at 200°C was found and weight loss about 29wt% was obtained. This value is much smaller than that 52wt% by gradual heating to 300°C. So larger amount of organic components is supposed to still remain in the precursor powder after pyrolysis at 200°C. Thus a comparison between the pyrolysis temperatures was considered to be important in order to investigate the effect of organics in precursor.
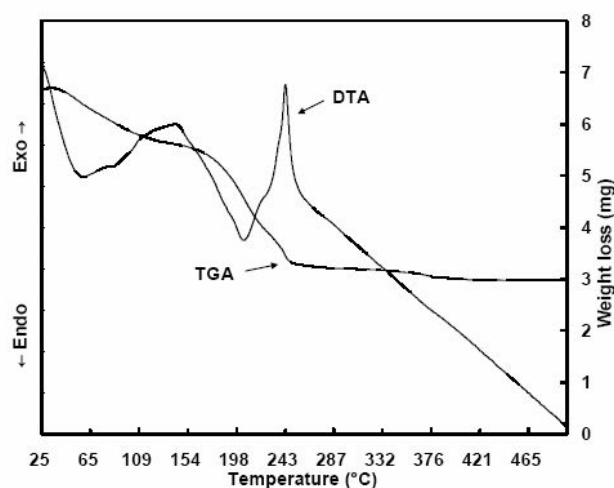

Fig. 1. TG-DTA curves of the starting sol after drying in oven at 50°C for 24 hrs.

On the basis of the structural analysis of isomorphic LiY(MoO$_4$)$_2$ [9], scheelite-type LEW has the following crystallographic properties: (i) the crystal structure belongs to a tetragonal system with its space group of I4$_1$/a, (ii) randomly distributed dodecahedra of LiO$_8$ and EuO$_8$ are surrounded by WO$_4$ tetrahedral units. Fig. 2 gives the XRD patterns of LEW as a function of pyrolysis temperature. All the samples are isostructural and belong to the tetragonal system of scheelite-type. In this work, isomorphic NaYW$_2$O$_8$ (JCPDS No. 48-886) is used to compare, since the crystal structure analysis of LEW has not been reported yet and NaYW$_2$O$_8$ exhibits an identical diffraction pattern to bulk LEW [11]. In this structure, W^{6+} occupies the tetrahedral sites constructed with O^{2-} composing WO$_4$$^{2-}$ anion complex. Li^{2+} is eight-coordinated with O^{2-}, forming a distorted cube. The dopant Eu^{3+} occupies the Li^{2+} site. Since there is no significant shift in the peak location, we can consider that the doped Eu^{3+} has little influence on the host structure.
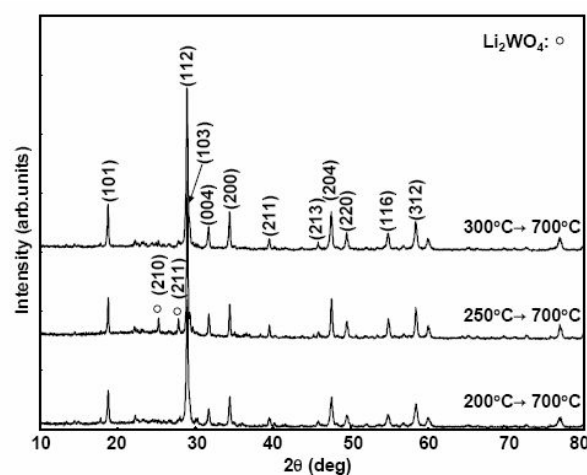

Fig. 2. XRD patterns of the annealed LEW powders as a function of pyrolysis temperature.

When the pyrolyzed gel was annealed at 700°C, only the scheelite-type LEW phase appeared, and no peaks from impurities were present. This result clearly indicated that sol-gel method effectively decreases the annealing temperature for obtaining the single phase of scheelite-type LEW.

The major diffraction peak at $2\theta \approx 29°$ (112) reflection and other diffraction peaks occurred at $2\theta \approx 18.8°$ (101), 31.7° (004), 34.4° (200) and 47.5° (204), corresponding to the LEW structure, as shown in Fig. 2. With an increase of pyrolysis temperature, the peak intensity increases, as shown in Table 1. This result can be explained by the fact that the precursor pyrolyzed at lower temperatures is assumed to contain some organics, as shown in Fig. 1. In this case crystallization may be suppressed by the residual organics during final annealing, since crystallization and decomposition of organic components proceeded concurrently. The LEW prepared by sol-gel and pyrolyzed at high temperature can be expected to have high crystallinity.

Table 1. Peak intensities of (112) reflection from annealed LEW

Pyrolysis te mperature	Intensity
200°C	2198
250°C	2703
300°C	3775

On the basis of XRD data, the lattice parameter has been estimated to be $a = 0.5201 \sim 0.5204$ and $c = 1.1268 \sim 1.1272$, as shown in Table 2. These values are similar to the reference value of $a = 0.5208$ and $c = 1.1282$ for bulk LEW [12].

Table 2. Lattice parameters for the annealed LEW as a function of pyrolysis temperature.

Lattice parameter	Pyrolysis temperature			Ref. [12]
	200°C	250°C	300°C	
a	0.5201	0.5201	0.5204	0.5208
c	1.1272	1.1268	1.1272	1.1282

Fig. 3 shows the FE-SEM image of annealed LEW powders at various pyrolysis temperatures. With an increase of pyrolysis temperature from 200°C to 250°C and 300°C, particle size increases. Crystal growth may be suppressed by residual organic components during the

final annealing, resulting in relatively small particle size for the annealed LEW at 200°C.
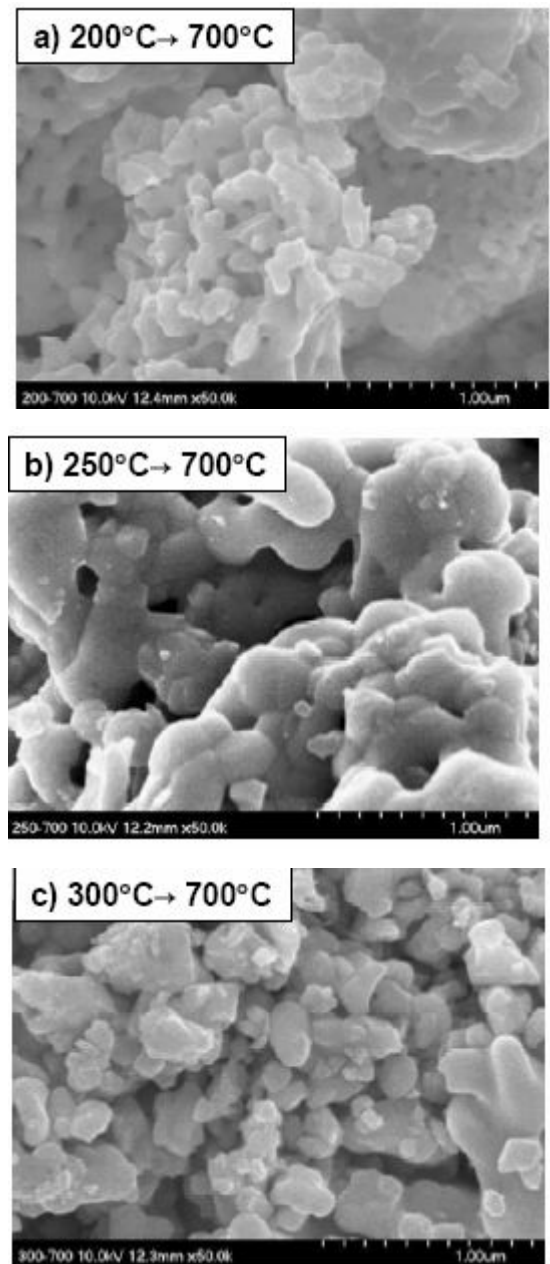

Fig. 3. FE-SEM images of the annealed LEW powders as a function of pyrolysis temperature.

The excitation and emission spectra of LEW excited by near-UV (395 nm) at ambient temperature as a function of pyrolysis temperature are illustrated in Fig. 4. The luminescence intensity of LEW increases with increasing pyrolysis temperature, which is because the crystallinity of LEW phosphor increases with increasing of pyrolysis temperature, as shown in XRD analysis.

The broad excitation curve near 250 nm is assigned as the charge-transfer band (CTB) originated from oxygen to

tungsten within the WO$_4^{2-}$ group, as discussed by Sivakumar and Varadaraju [13]. The Eu^{3+} excitation spectra of the LEW cover the ranges from long-wavelength UV to visible green-light region (300 ~ 500 nm). In the range from 300 to 500 nm, all samples show characteristic intra-configurational 4f-4f emissive transitions of Eu^{3+}: $^7F_0 \rightarrow {}^5D_4$ transition for 364 nm, $^7F_0 \rightarrow {}^5L_7$ transition for 384 nm, $^7F_0 \rightarrow {}^5L_6$ transition for 396 nm, $^7F_0 \rightarrow {}^5D_3$ transition for 418 nm, and the $^7F_0 \rightarrow {}^5D_2$ transition for 466 nm.
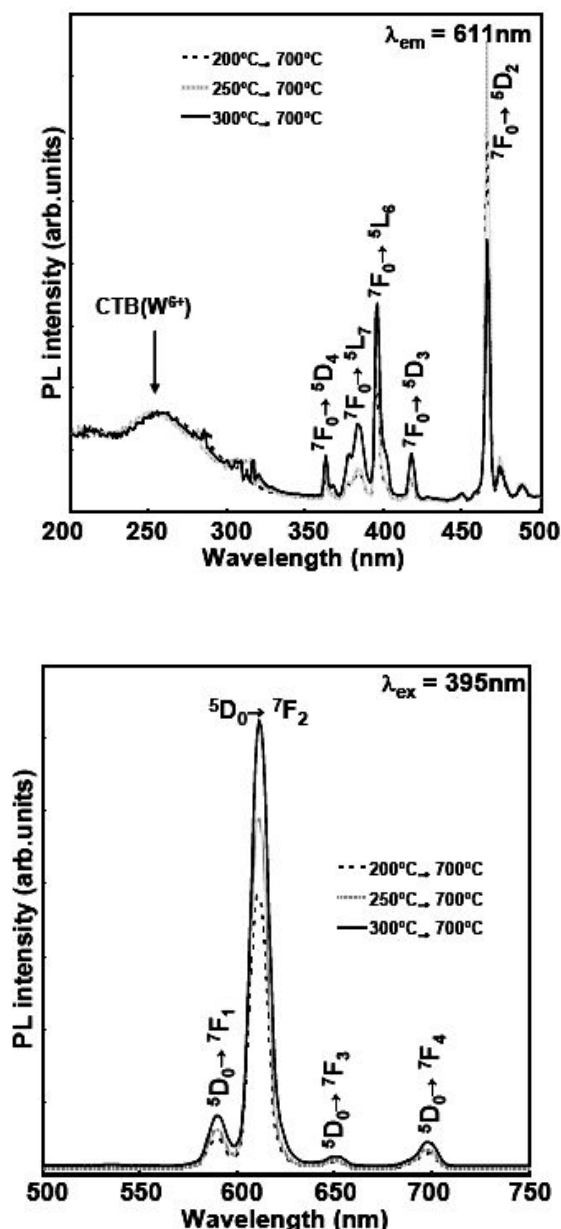

Fig. 4. Excitation and emission spectra of the annealed LEW as a function of pyrolysis temperature.

Between luminescent center and crystal lattice, two couplings are performed in luminescent materials. One is the strong coupling (WO$_4^{2-}$ group) with high Huang-Rhys factor. The other belongs to the weak coupling (Eu^{3+} ions) with low Huang-Rhys factor [14]. Generally the strong coupling of CTB (W^{6+}) is predominant, whereas the weak coupling of CTB (Eu^{3+}) is subordinate. When CTB (Eu^{3+}) is excited, the energy absorbed from charge-transfer state is efficiently transferred to Eu^{3+} ion by a non-radiative mechanism, and generate red-light emission of the $^5D_0 \rightarrow {}^7F_J$ transition of Eu^{3+}. However, in this work, CTB in 200 ~ 300 nm range for WO$_4^{2-}$ group is remarkably weak, compared with that of LiEuMo$_2$O$_8$ [10] and the f-f transitions of Eu^{3+} dominate the excitation process. Comparing the LEW phosphors prepared in this work, the Eu^{3+} transitions in LEW excitation spectra at high annealing temperature show more effective absorption at near-UV (396 nm) and blue (466 nm), and these wavelengths coincide with the those of commercial GaN-based LED.

Emission spectra according to the pyrolysis temperature are similar, corresponding to typical 4f levels specific transitions of Eu^{3+}. The main emission peak is $^5D_0 \rightarrow {}^7F_2$ transitions of Eu^{3+} at 615 nm, other transitions from the $^5D_0 \rightarrow {}^7F_1$, $^5D_0 \rightarrow {}^7F_3$ and $^5D_0 \rightarrow {}^7F_4$ located at 570 ~ 700 nm range are weak. The characteristic emission of WO$_4^{-2}$ in LEW is quenched absolutely and only red-light emission of Eu^{3+} appears. The strong emission peak around 615 nm and relatively weak peak around 699 nm is due to the electric dipole energy transition of $^5D_0 \rightarrow {}^7F_{2,4}$. The weak emissions of 592 nm and 651 nm are ascribed to the magnetic dipole transition of $^5D_0 \rightarrow {}^7F_{1,3}$. The electric-dipole allowed transition would be dominant when Eu^{3+} occupied the lattice site of noncentrosymmetric environment in the scheelite phases [15]. For this reason, the intensity of $^5D_0 \rightarrow {}^7F_{2,4}$ was found to be much stronger than that of $^5D_0 \rightarrow {}^7F_{1,3}$. When the pyrolysis temperature is increased, the LEW shows stronger red emission at 615 nm by exciting at near-UV wavelength of 395 nm. Comparing with the LEW pyrolyzed at 200°C, the sample pyrolyzed at 300°C has a high crstallinity, which is favorable to luminescent properties. Furthermore, doping of Eu^{3+} is more easy and effective in sol-gel process than traditional solid-state reaction since all of the starting materials are mixed at the molecular level.

4. Conclusions

Scheelite-type LEW phosphors for white-LED were prepared at various pyrolysis temperature by using a sol-gel method. The crystal structure, particle shape and luminescent properties under near-UV (395 nm) excitation of the phosphor have been investigated. In the emission spectra, the strongest emission is the electric dipole transition red emission $^5D_0 \rightarrow {}^7F_2$ (615 nm), while the magnetic dipole transition orange emission $^5D_0 \rightarrow {}^7F_{1,3}$ (592 and 651 nm) is subordinate. Comparing with the LEW pyrolyzed at 200°C, the sample pyrolyzed at 300°C has a high crystallinity, which is favorable to luminescent properties.

References

[1] S. Nakamura, T. Mukai, M. Senoh, J. Appl. Phys. **76**(12), 8189 (1994).

[2] C. H. Lu, H. C. Hong, and R. Jagannathan, J. Mater. Chem. **12**, 2525 (2002).

[3] Y. C. Kang, I. W. Lenggoro, S. B. Park, and K. Okuyama, Mater. Res. Bull. **35**, 789 (2000).

[4] T. Nishida, T. Ban, and N. Kobayashi, Appl. Phys. Lett. **82** (22), 3817 (2003).

[5] H. Wu, X. Zhang, C. Guo, J. Xu, and Q. Su, IEEE Photonics Technol. Lett. **17**(6), 1160 (2005).

[6] T. Odaki, K. Takagi, K. Hashimoto, and Y. Toda, J. Jpn. Soc. Colour Mater. **74**, 495 (2001).

[7] L. G. Van Uitert and L. F. Johnson, J. Chem. Phys. **44**, 3514 (1966).

[8] J. P. M. Van Vliet, G. Blasse, and L. H. Brixner, J. Solid State Chem. **76**, 160 (1988).

[9] R. Kasuya, T. Isobe, and S. Yamao, Jpn. J. Appl. Phys. **46**(9A), 5879 (2007).

[10] J. Wang, X. Jing, C. Yan, J. Lin, and F. Liao, J. Lumin. **121**, 57 (2006).

[11] P. V. Klevstov and R. F. Klevtsova, J. Struct. Chem. **18**, 339 (1977).

[12] E. Guermen, E. Deniels, and J. S. King, J. Chem. Phys. **55**, 1093 (1971).

[13] V. Sivakumar and U. V. Varadaraju, J. Electrochem. Soc. **152**, H168 (2005).

[14] S. Shi, X. Liu, J. Gao, and J. Zhou, Spectrochimica Acta A **69**, 396 (2008).

[15] C. H. Chiu, M. F. Wang, C. S. Lee, and T. M. Chen, J. Solid State Chem. **180**, 619 (2007).

_____

*Corresponding author: khwang@nambu.ac.kr